# Development of 3,4-dihydroisoquinolin-1(2H)-one derivatives for the Positron Emission Tomography (PET) imaging of σ2 receptors

**ARTICLE** *in* EUROPEAN JOURNAL OF MEDICINAL CHEMISTRY · SEPTEMBER 2013

Impact Factor: 3.45 · DOI: 10.1016/j.ejmech.2013.09.018 · Source: PubMed

European Journal of Medicinal Chemistry 69 (2013) 920–930

Contents lists available at ScienceDirect

European Journal of Medicinal Chemistry

journal homepage: http://www.elsevier.com/locate/ejmech

Original article

# Development of 3,4-dihydroisoquinolin-1(2*H*)-one derivatives for the Positron Emission Tomography (PET) imaging of $\sigma_2$ receptors

Carmen Abate [a, *], Svetlana V. Selivanova [b], Adrienne Müller [b], Stefanie D. Krämer [b], Roger Schibli [b], Roberta Marottoli [a], Roberto Perrone [a], Francesco Berardi [a], Mauro Niso [a], Simon M. Ametamey [b]

[a] *Dipartimento di Farmacia-Scienze del Farmaco, Università degli Studi di Bari ALDO MORO, Via Orabona 4, I-70125 Bari, Italy*
[b] *Center for Radiopharmaceutical Sciences, ETH Zurich, Zurich, Switzerland*

ARTICLE INFO

*Article history:*
Received 16 May 2013
Received in revised form
6 September 2013
Accepted 7 September 2013
Available online 20 September 2013

*Keywords:*
σ receptors
$\sigma_2$ receptors PET probe
6,7-Dimethoxytetrahydroisoquinoline
Dihydroisoquinolinone
PET

ABSTRACT

$\sigma_2$ Receptors are promising biomarkers for cancer diagnosis given the relationship between the proliferative status of tumors and their density. With the aim of contributing to the research of $\sigma_2$ receptor Positron Emission Tomography (PET) probes, we developed 2-[3-[6,7-dimethoxy-3,4-dihydroisoquinolin-2(1*H*)-yl]propyl]-3,4-dihydroisoquinolin-1(2*H*)-one (**3**), with optimal $\sigma_2$ pharmacological properties and appropriate lipophilicity. Hence, **3** served as the lead compound for the development of a series of dihydroisoquinolinones amenable to radiolabeling. Radiosynthesis for compound **26**, which displayed the most appropriate $\sigma_2$ profile, was developed and $\sigma_2$ specific binding for the corresponding [$^{18}$F]-**26** was confirmed by in vitro autoradiography on rat brain slices. Despite the excellent in vitro properties, [$^{18}$F]-**26** could not successfully image $\sigma_2$ receptors in the rat brain in vivo, maybe because of its interaction with P-gp. Nevertheless, [$^{18}$F]-**26** may still be worthy of further investigation for the imaging of $\sigma_2$ receptors in peripheral tumors devoid of P-gp overexpression.


## 1. Introduction

Sigma receptors are a unique pharmacologically defined family of proteins, which has been thus far divided into $\sigma_1$ and $\sigma_2$ subtypes. The $\sigma_1$ receptors, which were purified and cloned in 1996 [1], are the most well characterized. A chaperone function has been assigned to this protein and increasing lines of evidence demonstrate that $\sigma_1$ proteins are involved in the intracellular signaling through the modulation of intracellular $Ca^{2+}$ levels via inositol 1,4,5-trisphosphate ($IP_3$) receptors [2]. A role in neuroprotection and neuroplasticity has also been shown for this subtype which seems to be involved in a series of Central Nervous System (CNS) pathologies such as anxiety, depression, schizophrenia, drug addiction, Parkinson's and Alzheimer's diseases so that $\sigma_1$ receptor appears as an interesting therapeutic target [3].

The $\sigma_2$ receptor gene has yet to be cloned. $\sigma_2$ receptor structure, intracellular localization and pathways activated are still unclear. Diverse attempts to isolate this receptor led to contradictory results [4], and only recently $\sigma_2$ receptors have been proposed as the progesterone receptor membrane component 1 (PGRMC1) protein [5,6]. Nevertheless, interest in $\sigma_2$ receptors is on the increase because of the important therapeutic potentials that are foreseen for this subtype [7–9]. In fact, the $\sigma_2$ subtype in particular, is overexpressed in several tumor cell lines and its activation with $\sigma_2$ agonists leads cancer cells to apoptotic pathways [10]. Diverse $\sigma_2$ agonists have been demonstrated to be powerful anticancer agents in vitro as well as in tumor xenografts in vivo [11–13].

In addition, $\sigma_2$ subtype has been validated as an endogenous biomarker for cancer diagnosis as a relationship between the proliferative status of tumors and the density of $\sigma_2$ receptors has been demonstrated [14]. A clinical study (NCT00968656A) has just been completed with fluorine-18 radiolabeled (*N*-[4-(6,7-dimethoxy-3,4-dihydro-1*H*-isoquinolin-2-yl)butyl]-2-(2-fluoroethoxy)-5-iodo-3-methoxybenzamide (**ISO-1**) for the assessment of cellular proliferation in tumors by Positron Emission Tomography (PET) [15]. **ISO-1** belongs to a series of flexible benzamides which were

*Abbreviations:* Calcein-AM, acetoxymethylester of calcein; BBB, blood–brain barrier; CNS, central nervous system; DMEM, Dulbecco's modified eagle medium; DTG, 1,3-di-o-tolyl-guanidine; $IP_3$, inositol 1,4,5-trisphosphate; MDCK-MDR1, Madin Darby canine kidney cells transfected with the human MDR1 gene; PET, Positron Emission Tomography; P-gp, P-glycoprotein; $P_{app}$, apparent permeability; PGRMC1, progesterone receptor membrane component 1.

* Corresponding author. Tel.: +39 080 5442750; fax: +39 080 5442231.
*E-mail address:* carmen.abate@uniba.it (C. Abate).

0223-5234/$ – see front matter © 2013 Elsevier Masson SAS. All rights reserved.
http://dx.doi.org/10.1016/j.ejmech.2013.09.018

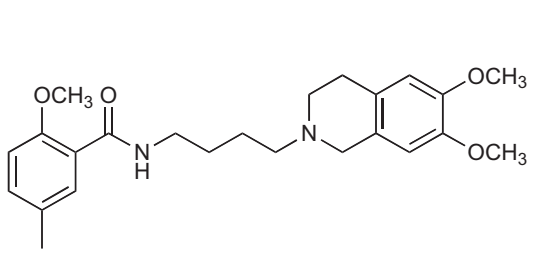


**1**, RHM-1

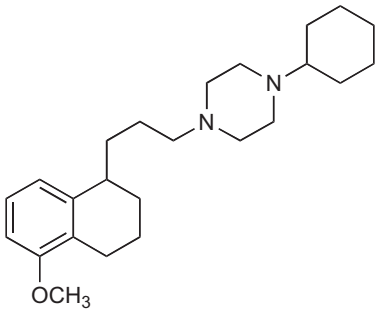


**2**, PB28

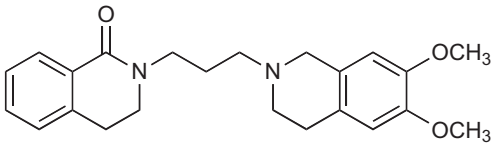


**3**

**Fig. 1.** $\sigma_2$ receptors reference compounds.

generated using the $\sigma_2$ receptor high-affinity ligand 5-methyl-2-methoxy-*N*-[4-(6,7-dimethoxy-3,4-dihydro-1*H*-isoquinolin-2-yl) butyl]benzamide (**1**, RHM-1; Fig. 1) as the lead compound. A few high $\sigma_2$ affinity and selectivity radioligands belonging to this series provided a clear image of diverse solid tumors with optimal tumor uptake which depended upon the log *P* values of the radioligands [16,17].

With the aim of contributing to the research of $\sigma_2$ receptor PET probes, we developed a series of compounds as hybrids of one of the highest affinity $\sigma_2$ ligands (1-cyclohexyl-4-[3-(5-methoxy-1,2,3,4-tetrahydronaphthalen-1-yl)-n-propyl]piperazine **2** PB28; Fig. 1) [18,19], and one of the best flexible benzamides (**1**, Fig. 1) [20]. Dihydroisoquinolinone derivative 2-[3-[6,7-dimethoxy-3,4-dihydroisoquinolin-2(1*H*)-yl]propyl]-3,4-dihydroisoquinolin-1(2*H*)-one (**3**, Fig. 1) displayed an optimal $\sigma_2$ pharmacological profile together with an appropriate lipophilicity value. In addition (and in contrast to flexible benzamides), a rather weak interaction of **3** with the P-glycoprotein (P-gp) [21], suggested that this class of compounds might be well suitable to selectively visualize $\sigma_2$ receptors in P-gp-overexpressing tumors. Therefore, 3,4-dihydroisoquinolin-1(2*H*)-one **3** served as a lead compound for the development of a series of dihydroisoquinolinone derivatives whose functionalization with methoxy, fluoroethoxy or fluorine could easily lead to the development of corresponding carbon-11 or fluorine-18 radiolabeled ligands for PET imaging. Radiosynthesis for compound [$^{18}$F]-**26**, which displayed the best $\sigma_2$ pharmacological profile was developed and prior to using $\sigma_2$-positive tumor-expressing animals, a preliminary study involving in vitro autoradiography on rat brain slices and biodistribution in rats were performed to evaluate the specificity of [$^{18}$F]-**26** binding to $\sigma_2$ receptors.

## 2. Chemistry

The synthesis of final compounds herein reported is depicted in Scheme 1. The synthetic pathway leading to [$^{18}$F]-**26** is depicted in Schemes 2 and 3. All the substituted 3,4-dihydro-isoquinolinones **10**–**15** were obtained from the corresponding indanones except for intermediate 3,4-dihydro-6-methoxy-isoquinolin-1(2*H*)-one **16** (Scheme 1) which was obtained, by cyclization of the ethyl-3-methoxyphenethylcarbamate as previously reported [21].

7-Methoxy-indan-1-one **4** was obtained starting from 3-(2-bromo-5-methoxyphenyl)propanoic acid [22]. Cyclization of this latter compound in polyphosphoric acid provided 4-Br-5-methoxy-indan-1-one, and its debromination led to indanone **4** with a little change of the procedure already reported [23]. Indanon-1-ones **8** and **9** were obtained by alkylation of the 5-hydroxy-indan-1-one **5** with $CH_3I$ or with 2-fluoroethyl-4-methylbenzenesulfonate [24] respectively, although the former compound was commercially available. Indan-1-ones **4**–**9** treated with $NaN_3$ in HCl or in $Cl_3CCOOH$ led to key 3,4-dihydro-isoquinolinones **10**–**15** [25]. 5-Hydroxy derivative **10**, obtained by the corresponding indanone **5** according to a previously reported procedure [25], was benzylated by the use of benzylbromide and $K_2CO_3$ to afford the already known 5-benzyl-3,4-dihydro-isoquinolinone **17** [26], through a different procedure. Alkylation of 3,4-dihydro-isoquinolinones **11**–**17** with 1-Bromo-3-chloropropane using NaH as a base afforded 2-(3-chloropropyl)-3,4-dihydroisoquinolin-1(2*H*)-one derivatives (**18**–**24**) whose reaction with 6,7-dimethoxy-3,4-dihydro-1*H*-isoquinoline led to final compounds **25**, **26**, **28**–**31** and 5-benzyl intermediate **27** (Scheme 1).

Debenzylation of this last compound in the presence of $H_2$ and Pd on activated carbon 10% as the catalyst furnished intermediate **32** which was subsequently reacted with 2-bromoethylacetate to afford intermediate **33**. Hydrolysis of the acetyl group in basic medium led to the 2-ethoxy-ethanol intermediate **34**. Reaction of this last compound with p-toluensulfonyl chloride gave the precursor **35** which was then used for the radiolabeling to afford [$^{18}$F]-**26.** All of the final amine compounds were converted into their hydrochloride salts with gaseous HCl, in anhydrous diethyl ether except for compound **29** which could not be recrystallized and therefore it was analyzed as free base. Physical properties of the hydrochloride salts are listed in the Table of Physical Properties of Novel Compounds in the Supporting information.

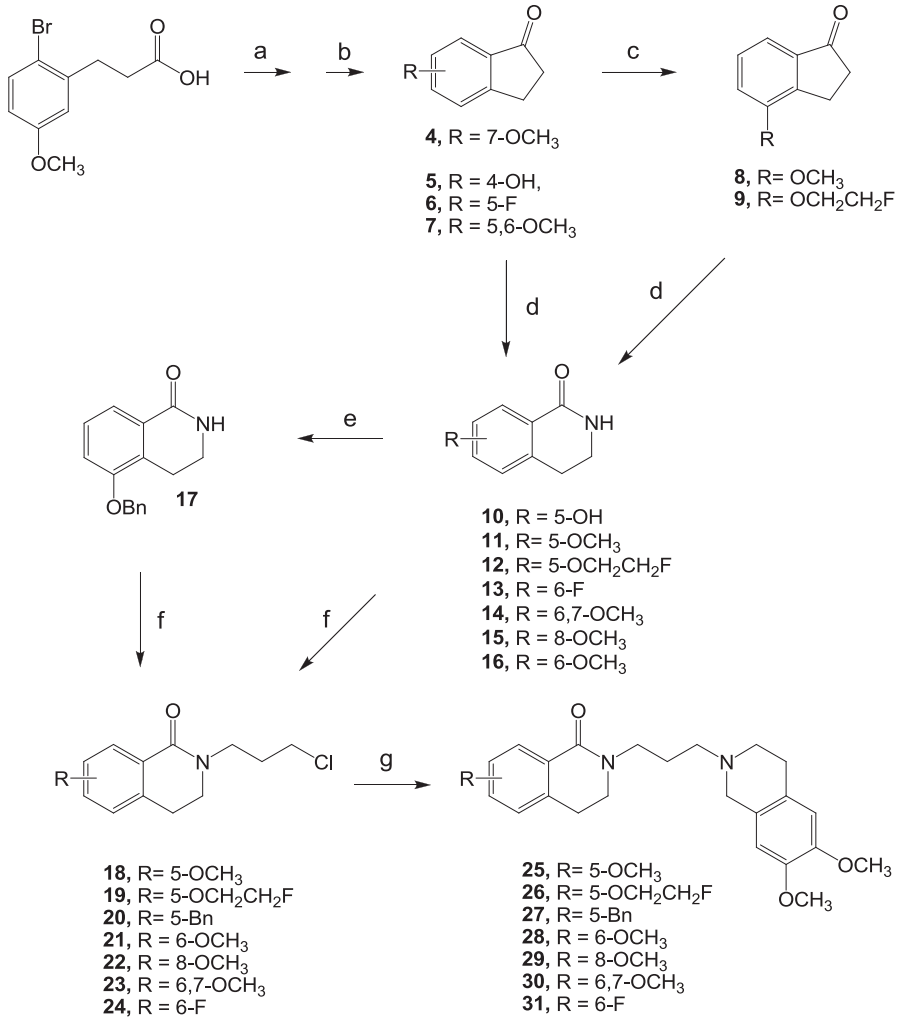


**Scheme 1.** Reagents and conditions: a) Polyphosphoric acid, 60 °C, 1 h (synthesis of intermediate **4**); b) $H_2$, Pd/C 10%, NaOAc, EtOH, RT, 4 h (synthesis of intermediate **4**); c) MeI or 2-Fluoroethyl-4-methylbenzenesulfonate, $K_2CO_3$, Acetone, reflux, 6 h or 36 h respectively; d) $NaN_3$, HCl 37%, RT, 12 h; e) Benzylbromide, $K_2CO_3$, Acetone, reflux, 18 h; f) 1-Bromo-3-chloropropane, NaH, DMF, RT, 30 min (Procedure A); 1-Bromo-3-chloropropane, NaH, THF, reflux, 18 h (Procedure B); g) 6,7-Dimethoxy-1,2,3,4-tetrahydroisoquinoline hydrochloride, $K_2CO_3$, reflux, 18 h.

## 3. Results and discussion

### 3.1. $\sigma_1$ and $\sigma_2$ receptor affinities

Results from binding assays are expressed as inhibition constants ($K_i$ values) in Table 1. The $K_i$ values at the $\sigma_1$ subtype for the present series of compounds are in the micromolar range generally presenting a 3- to 4-fold reduction in the affinity compared to the unsubstituted isoquinolinone derivative **3** ($K_i$ = 709 nM). Exceptions to this were 6-substituted compounds: 6-methoxy- and 6-fluoro- derivatives **28** and **31** exhibited a 2-fold improvement in the affinity ($K_i$ values = 402 nM and 311 nM respectively), compared to **3**. These results suggested that independently of their electronic effects, substituents at the isoquinolinone 6-position are less detrimental for the interaction with the $\sigma_1$ receptor. On the other hand, the presence of an electron-donating methoxy group in 5- or 7- or 8- position of the isoquinolinone benzene ring exerted a similar decrease in the $\sigma_1$ receptor binding (compounds **25**, **26**, **29** and **30**). The $K_i$ values at the $\sigma_2$ subtype for the newly synthesized compounds ranged from 3.56 nM to 20.1 nM (compounds **31** and **30** respectively) confirming the template of the 6,7-dimethoxytetrahydroisoquinoline linked to benzamides as appropriate in conferring remarkable $\sigma_2$ receptor affinity and selectivity. The presence of either an electron-donating (methoxy) or withdrawing substituent (fluorine) did not alter the affinity at the $\sigma_2$ receptor compared to the un-substituted lead-compound **3** as long as the group was introduced in 5- or 6-position of the benzene ring (compound **25**, **28** and **31**, $\sigma_2$ $K_i$ values = 4.24 nM, 6.16 nM and 3.56 nM respectively). The presence of the methoxy group in 7- or 8- position (**30** and **29**) of the 3,4-dihydroisoquinolinone system led to a slight reduction (around 4-fold) of the affinity at the $\sigma_2$ receptor. The presence of both the electron-donating (methoxy) and electron-withdrawing (fluorine) substituents was only explored for the 6-position of the benzene ring, where no electronic effect was detected compared to the unsubstituted **3**. 5-Methoxy-substituted **25** emerged as the most $\sigma_2$-selective ligand (574-fold) with a selectivity 4-fold higher compared to the lead compound **3**. Therefore, we identified the 5-methoxy-substitution of the 3,4-dihydroisoquionolinone system as a key feature to preserve high $\sigma_2$ selectivity. Introduction of $^{11}C$ into the 5-methoxy group would be one of the possible routes for the radiolabeling. However, the half-life of the $^{11}C$ radioisotope (20 min), prompted us to develop the corresponding 2-fluoroethoxy derivative **26** which displayed a lower but yet

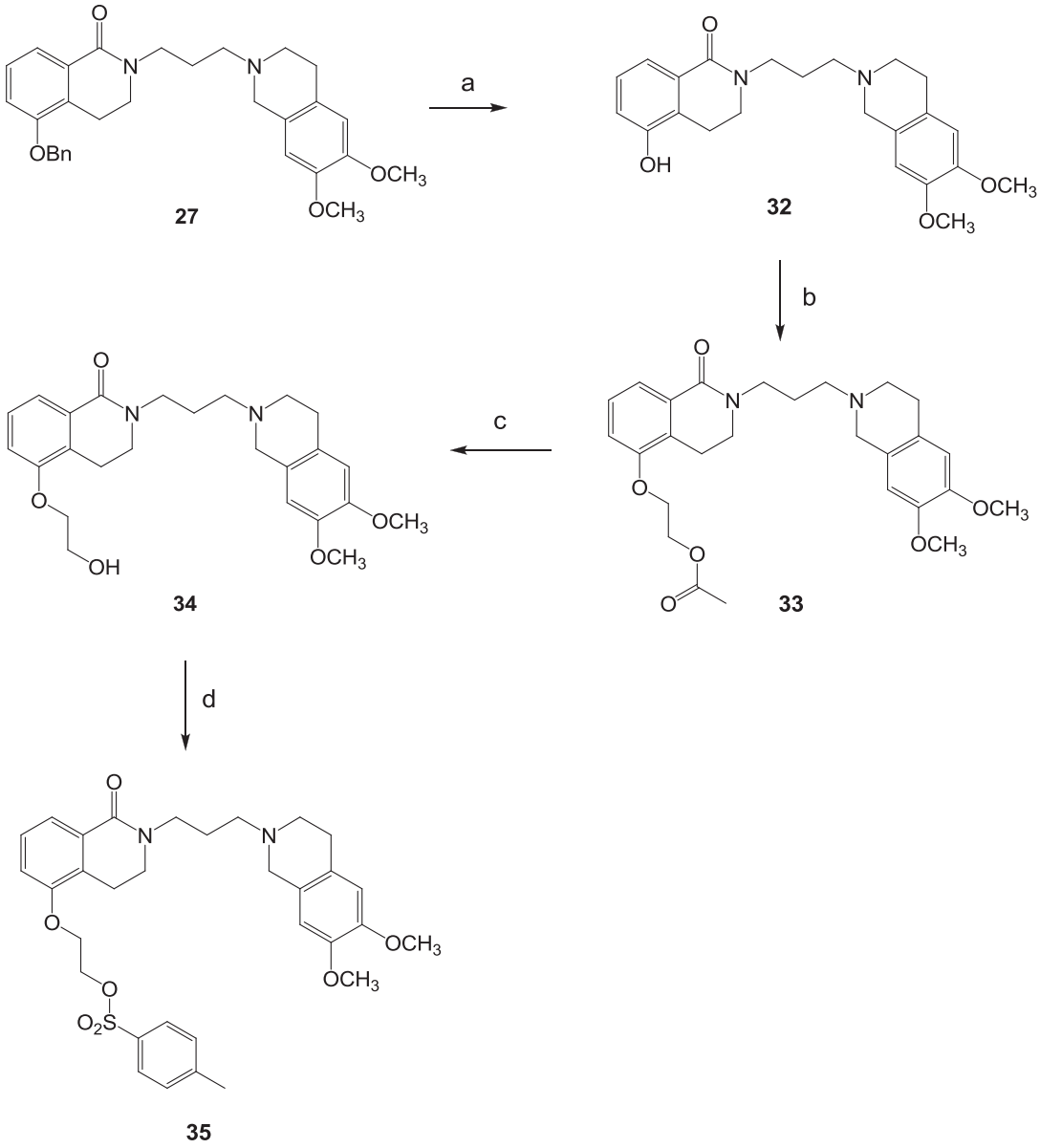


**Scheme 2.** Reagents and conditions: a) $H_2$ 10 atm, Pd/C 10%, EtOH, RT, 12 h; b) 2-Bromoethylacetate, $K_2CO_3$, Acetone, reflux, 24 h; c) NaOH, MeOH/$H_2O$, RT, 18 h; d) TsCl, $NEt_3$, $CH_2Cl_2$, RT, 1 h.

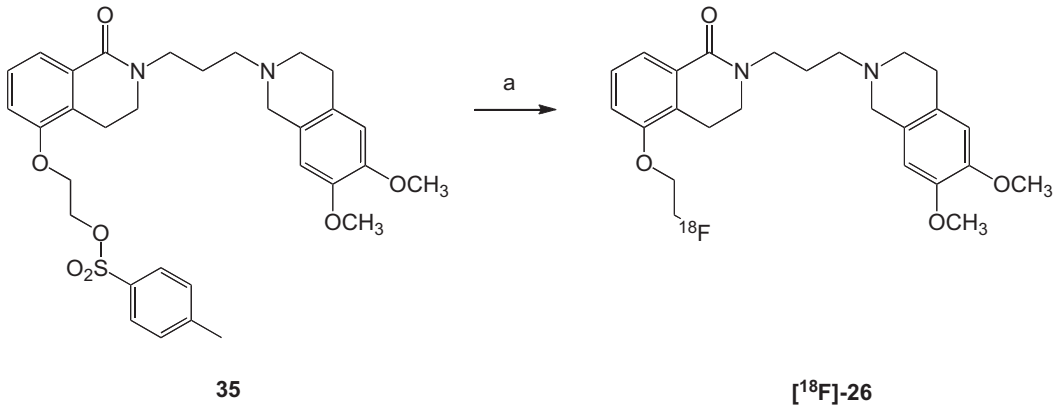


**Scheme 3.** Radiolabeling with $^{18}F$. Reagents and conditions: a) [$^{18}F$]-KF, $K_2CO_3$, $CH_3CN$, 100 °C, 10 min.

**Table 1**
Binding data of novel compounds at σ receptors.

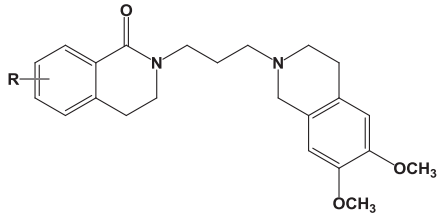


| Compd | R | $K_i \pm$ SEM (nM)[a] | | |
|---|---|---|---|---|
| | | $\sigma_1$ | $\sigma_2$ | $\sigma_1/\sigma_2$ |
| **3**[b] | H | 709 ± 133 | 4.74 ± 0.74 | 149 |
| **25** | 5-$OCH_3$ | 2435 ± 995 | 4.24 ± 0.84 | 574 |
| **26** | 5-$OCH_2CH_2F$ | 3095 ± 750 | 9.24 ± 2.55 | 330 |
| **28** | 6-$OCH_3$ | 402 ± 7 | 5.74 ± 0.42 | 70 |
| **29** | 8-$OCH_3$ | 1628 ± 61 | 16.3 ± 0.8 | 101 |
| **30** | 6,7-$OCH_3$ | 2567 ± 162 | 20.1 ± 2.5 | 127 |
| **31** | 6-F | 311 ± 8 | 3.56 ± 0.4 | 87 |
| (+)-Pentazocine | | 3.0 ± 0.21 | | |
| DTG | | | 25.7 ± 1.41 | |

[a] Values are the means of $n \geq 3$ separate experiments, in duplicate.
[b] From Ref. [20].

appreciable $\sigma_2$ receptor affinity ($K_i = 9.24$ nM) compared to **25**, and a high $\sigma_2$-selectivity (330-fold). This promising result encouraged us to further study this compound as PET radiotracer. For this purpose, we extended the binding of compound **26** to more receptors, as well as interaction at the P-gp was studied, so that possible and misleading interaction with other targets might be predicted.

### 3.2. Compound **26**: affinity at $\alpha_1$, $5HT_7$ and $5HT_{1a}$ receptors, activity at P-gp and apparent permeability ($P_{app}$)

Binding of **26** towards other CNS receptors such as $\alpha_1$, $5HT_7$ and $5HT_{1a}$ was studied, and results are expressed as $K_i$ values in Table 2. Affinity at both the serotonin receptors was low ($K_i$ values > 1000 nM), as well as at the α-adrenergic receptor ($K_i = 764$ nM), supporting the $\sigma_2$-selectivity of this compound. Also, interaction with P-gp was measured through the Calcein-AM experiment in the P-gp overexpressing cell line MDCK-MDR1. Compound **26** displayed a moderate interaction with P-gp ($EC_{50} = 5$ μM, Table 2), but stronger than the interaction of the lead compound **3** ($EC_{50} = 12$ μM). The Apparent Permeability ($P_{app}$) in Caco-2 cell monolayer was determined in order to predict the Blood Brain Barrier (BBB) permeation of **26**, but the result obtained was borderline. The flux of the compound from basolateral to apical (BA) represents the passive transport, whereas the flux from apical to basolateral (BA) represents the active transport, and in agreement to the current classification, compound is a P-gp inhibitor for BA/AB < 2; compound is a P-gp substrate for BA/AB > 2. Compound **26** displayed BA/AB = 2.58 (Table 2).

**Table 2**
Compound **26**: binding data at $5HT_{1a}$, $5HT_7$ and $\alpha_1$ receptors, P-gp activity and apparent permeability ($P_{app}$).

| Compd | $K_i \pm$ SEM (nM)[a] | | | $EC_{50}$ (μM)[a] | (BA/AB)[a] |
|---|---|---|---|---|---|
| | $5HT_{1a}$ | $5HT_7$ | $\alpha_1$ | P-gp | $P_{app}$ |
| **26** | >1000 | >1000 | 764 ± 98 | 5.0 ± 0.8 | 2.58 |
| 5-HT | 9.5 ± 1.1 | | | | |
| 5-CT | | 0.4 ± 0.05 | | | |
| Phentolamine | | | 15.2 ± 1.2 | | |
| MC18 | | | | 1.1 ± 0.2 | |

[a] Values are the means of $n \geq 3$ separate experiments, in duplicate.

Since the results from Calcein-AM experiment and from the apparent permeability ($P_{app}$) determination suggested could not allow to undoubtedly predict whether the compound may overcome BBB to bind $\sigma_2$ receptors, we developed the corresponding [$^{18}$F]-**26** to test its suitability as PET radiotracer, given the encouraging $\sigma_2$-binding profile of the compound.

### 3.3. Radiosynthesis

One step radiolabeling with $^{18}$F was achieved via aliphatic nucleophilic substitution of tosyl leaving group in the precursor molecule (**35**). The reaction between precursor (2.4 mg, 4 μmol) and dry $^{18}$F-fluoride was accomplished in anhydrous acetonitrile at 100 °C for 10 min. The product was purified by semi-preparative HPLC and formulated for biological experiments. Decay corrected radiochemical yield was 34.3 ± 1.5% and the total synthesis time was ~90 min. Radiochemical purity exceeded 98% and specific activity was in a range of 75–88 GBq/μmol. Typically, ~8 GBq of the formulated ready for in vivo application product could be produced starting with ~55 GBq $^{18}$F-fluoride. No attempts were made to optimize the reaction yield since produced amount of [$^{18}$F]-**26** was sufficient for our studies.

### 3.4. In vitro autoradiography

To evaluate binding of [$^{18}$F]-**26** to $\sigma_2$ receptors in vitro, we performed autoradiography using rat brain slices. [$^{18}$F]-**26** showed heterogeneous accumulation clearly delineating various brain regions (Fig. 2). Maximal binding was detected in cerebral cortex and hippocampus. High radioactivity accumulation was also observed in cerebellum. Overall, the binding pattern was consistent with binding of a known $\sigma_2$ radioligand, [$^3$H]-Lu28-179 [27]. Binding of [$^{18}$F]-**26** was blocked when rat brain slices were incubated with [$^{18}$F]-**26** in the presence of 90 μM haloperidol. The binding was also diminished in a dose-dependent manner by co-incubation with non-radioactive analog **26**: at 0.9 μM, binding was disrupted only partially, while blocking with 90 μM of **26** had a similar effect as blocking with 90 μM haloperidol. Our data thus confirm the specificity of [$^{18}$F]-**26** binding to $\sigma_2$ receptors in rat brain in vitro.

### 3.5. PET imaging in the rat brain

PET imaging showed a fast washout of [$^{18}$F]-**26** from rat brain. Virtually, no radioactivity accumulation was visible during 0–90 min scan after tracer injection (Fig. 3). Derived time–activity curves (TACs) showed elevated radioactivity levels in cerebral cortex, olfactory, and cerebellum, which is in agreement with the autoradiography results. However, radioactivity levels in hippocampus were not higher than in the remaining brain regions, in contrast to the autoradiography data. A PET scan under blocking conditions with 1 mg/kg haloperidol revealed similar TACs (data not shown). The increased radioactivity in cortex, olfactory and cerebellum under baseline and blocking conditions may result from spill over from the periphery rather than $\sigma_2$ receptor-related accumulation. The TACs may represent blood radioactivity, without any transfer of [$^{18}$F]-**26** across the BBB, despite its relatively high estimated lipophilicity (clogP 3.5 [28]). As data standing, the ambiguous interaction with P-gp that we evaluated through Calcein-AM and $P_{app}$ experiments, resulted in the absence of BBB passage, suggesting that **26** may be a P-gp substrate, strongly effluxed out of the CNS. Another speculation on possible reasons for the discrepancy between the in vitro and in vivo data and for the low brain SUV in general, is that [$^{18}$F]-**26** could undergo rapid biotransformation to radiometabolite(s) with low BBB permeation. The slight steady but unspecific increase in brain radioactivity could

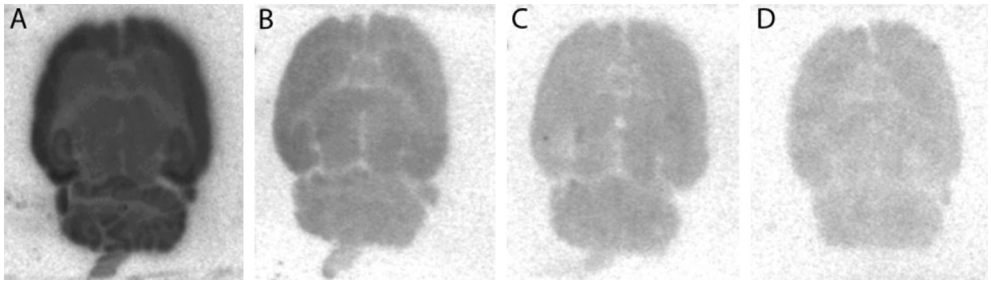


**Fig. 2.** In vitro autoradiography using rat brain slices under baseline (A) and blocking (B–D) conditions. A: 9 nM [$^{18}$F]-**26** solution; B: co-incubation of 9 nM [$^{18}$F]-**26** and 0.9 μM unlabeled **26**; C: co-incubation of 9 nM [$^{18}$F]-**26** and 90 μM unlabeled **26**; D: co-incubation of 9 nM [$^{18}$F]-**26** plus 90 μM haloperidol.

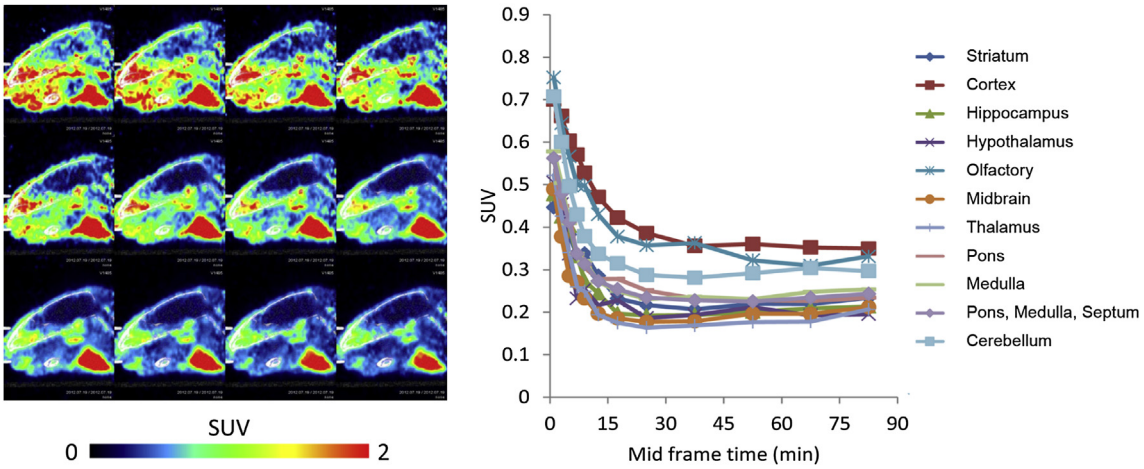


**Fig. 3.** Time series of a rat's head PET scan (left) and time–activity curves (right) from 0 to 90 min after injection of [$^{18}$F]-**26**.

result from radiometabolite(s). In many cases, defluorination of PET tracers precludes successful imaging. In this study, we did not observe any appreciable radioactivity accumulation in the bones, which confirmed that no free $^{18}$F-fluoride was released by [$^{18}$F]-**26**. Extensive binding at the blood macromolecule, that is another possible reason for low BBB permeation, was excluded since the TRANSILXL assay predicted only a low fraction (84%) of **26** bound to plasma proteins (data not shown) [29].

## 4. Conclusion

We synthesized a series of dihydroisoquinolinone derivatives and evaluated their binding properties to σ receptors. Selected compound, **26**, showed high affinity and selectivity towards $\sigma_2$, but ambiguous interaction with the efflux pump P-gp. After radiolabeling with $^{18}$F, **26** was evaluated as a potential PET tracer. Despite encouraging results from in vitro autoradiography, [$^{18}$F]-**26** was not successful in imaging $\sigma_2$ receptors in the rat brain in vivo, maybe because its BBB passage is hampered by interaction with P-gp, although other reasons may not be excluded. Nevertheless, the tracer may still be worthy of further investigation for the imaging of $\sigma_2$ receptors in peripheral tumors devoid of P-gp overexpression.

## 5. Chemistry: materials and methods

### 5.1. Chemistry

Both column chromatography and flash column chromatography were performed with 60 Å pore size silica gel as the stationary phase (1:30 w/w, 63–200 μm particle size, from ICN and 1:15 w/w, 15–40 μm particle size, from Merck respectively). Melting points were determined in open capillaries on a Gallenkamp electrothermal apparatus. Purity of tested compounds was established by combustion analysis, confirming a purity ≥ 95%. Elemental analyses (C, H, N) were performed on an Eurovector Euro EA 3000 analyzer; the analytical results were within ±0.4% of the theoretical values. $^1$H NMR (300 MHz) and $^{13}$C NMR (75 MHz) spectra were recorded on a Mercury Varian: $CDCl_3$ was used as solvent to record $^1$H NMR on intermediate and final compounds as free basis and the following data were reported: chemical shift ($\delta$) in ppm, multiplicity (s = singlet, d = doublet, t = triplet, m = multiplet), integration and coupling constant(s) in Hertz. $CD_3OD$ was used as solvent to record $^{13}$C NMR on hydrochloride salts of final compounds where reported and chemical shift ($\delta$) in ppm were reported. Recording of mass spectra was done on an Agilent 6890–5973 MSD gas chromatograph/mass spectrometer and on an Agilent 1100 series LC-MSD trap system VL mass spectrometer; only significant $m/z$ peaks, with their percentage of relative intensity in parentheses, are reported. Infrared spectra were recorded on a Perkin–Elmer, Spectrum one, FTIR. Chemicals were from Aldrich and Acros, and were used without any further purification. Radiolabeling reactions were monitored by ultra-performance liquid chromatography (UPLC). The system was Acquity UPLC from Waters, equipped with a built-in PDA detector and an additional FlowStar LB 513 radiodetector (Berthold Technologies) and a reversed-phase Acquity BEH C18 column (particle size 1.7 μm, 100 × 2.1 mm). The mobile phase consisted of a gradient of acetonitrile in aqueous 50 mM $NH_4COOH$ buffer (pH 4.45) from 5 to 65% over 2 min at a flow rate 0.7 mL/min. Semi-preparative HPLC for radiolabeled product purification was carried out on an HPLC

system equipped with a Merck-Hitachi L-6200A Intelligent pump, a 5 mL injection loop, a Knauer Variable Wavelength Monitor UV-detector, and an Eberline RM-14 radiodetector on a reversed-phase Waters μBondapack C18, 10 μm, 125 Å, 300 × 7.8 mm column. The mobile phase consisted of acetonitrile and 50 mM $NH_4COOH$ buffer (pH 4.45). The gradient was: 0–10 min, isocratic 5% acetonitrile; 10–40 min, 5% → 65% acetonitrile and eluted at 4 mL/min flow rate. UV-absorbance was detected at 235 nm. Analytical HPLC was an Agilent 1100 series system equipped with a Raytest Gabi Star radiodetector. Analytical reversed-phase column was Agilent Eclipse XDB-C18, particle size 5 μm, 50 × 4.6 mm. A gradient of acetonitrile in aqueous 50 mM $NH_4COOH$ buffer (pH 4.45) from 10% to 65% over 13 min at a flow rate of 1 mL/min was used.

### 5.2. General procedures for the synthesis of alkyl chloride derivatives

#### 5.2.1. General procedure A

To a suspension of NaH (0.11 g, 4.5 mmol) in DMF (10 mL), a solution in DMF (5 mL) of the appropriate 3,4-dihydroisoquinolin-1-one (1.8 mmol), was added in a dropwise manner, at 0 °C under a stream of $N_2$. After 15 min, 1-bromo-3-chloropropane was added in a dropwise manner and the mixture was allowed to warm to room temperature and was kept under stirring for 30 min. After cooling to 0 °C $H_2O$ was added and the solvent was removed under reduced pressure. The residue was taken up with water and extracted with AcOEt (3 × 10 mL). The organic layers were collected, dried over $Na_2SO_4$ and evaporated under reduced pressure. The crude residue was purified by column chromatography with $CH_2Cl_2$/AcOEt (1:1) as eluent.

*5.2.1.1. 2-(3-Chloropropyl)-5-methoxy-3,4-dihydroisoquinolin-1(2H)-one (**18**).* Compound **18** was obtained as yellow oil (0.26 g, 58%); $^1$H NMR $\delta$ = 2.10–2.19 (m, 2H, C*H*$_2$CH$_2$Cl), 2.97 (*t*, 2H, *J* = 6.6 Hz, ArCH$_2$), 3.46–3.75 (m, 6H, 2 CH$_2$N, and CH$_2$Cl), 3.85 (s, 3H, OCH$_3$), 6.98 (d, 1H, *J* = 8 Hz, aromatic), 7.26–7.32 (m, 1H, aromatic), 7.68 (d, 1H, *J* = 7.7 Hz, aromatic); LC–MS (ESI$^+$) *m/z*: 276 [M + H]$^+$; LC–MS–MS 276; 218.

*5.2.1.2. 2-(3-Chloropropyl)-5-(2-fluoroethoxy)-3,4-dihydroisoquinolin-1(2H)-one (**19**).* Compound **19** was obtained as yellow oil (0.25 g, 55%); $^1$H NMR $\delta$ = 2.10–2.19 (m, 2H, C*H*$_2$CH$_2$Cl), 3.02 (*t*, 2H, *J* = 6.6 Hz, ArCH$_2$), 3.47–3.71 (m, 6H, 2 CH$_2$N, and CH$_2$Cl), 4.18–4.38 (m, 2H, CH$_2$O), 4.65–4.86 (m, 2H, CH$_2$F), 6.97 (d, 1H, *J* = 8.2 Hz, aromatic), 7.26–7.31 (m, 1H, aromatic), 7.72 (d, 1H, *J* = 7.8 Hz, aromatic); GC–MS *m/z* 285 (M$^+$, 12), 250 (100), 222 (57).

*5.2.1.3. 2-(3-Chloropropyl)-5-benzyloxy-3,4-dihydroisoquinolin-1(2H)-one (**20**).* Compound **20** was obtained as yellow oil (0.34 g, 58%); GC–MS *m/z* 329 (M$^+$, 12), 91 (100); LC–MS (ESI$^+$) *m/z* 330 [M + H]$^+$; *m/z* 352 [M + Na]$^+$.

#### 5.2.2. General procedure B

To a solution of the appropriate 3,4-dihydroisoquinolin-1-one (1.2 mmol) in THF, NaH (0.07 g, 3 mmol) was added at 0 °C under a stream of $N_2$. After 10 min, the mixture was allowed to warm to room temperature and 1-bromo-3-chloropropane was added in a dropwise manner. The reaction mixture was heated to reflux overnight. After cooling $H_2O$ was added and the mixture was extracted with $Et_2O$ (3 × 5 mL), the organic layers were collected, dried over $Na_2SO_4$ and evaporated under reduced pressure. The crude residue was purified by column chromatography with $CH_2Cl_2$/AcOEt (9:1) as eluent.

*5.2.2.1. 2-(3-Chloropropyl)-6-methoxy-3,4-dihydroisoquinolin-1(2H)-one (**21**).* Compound **21** was obtained as yellow oil (0.12 g, 39%); $^1$H NMR $\delta$ = 2.09–2.18 (m, 2H, C*H*$_2$CH$_2$Cl), 2.97 (*t*, 2H, *J* = 6.5 Hz, ArCH$_2$), 3.57–3.70 (m, 6H, 2 CH$_2$N, and CH$_2$Cl), 3.84 (s, 3H, OCH$_3$), 6.66 (d, 1H, *J* = 2.7 Hz, aromatic), 6.84 (dd, 1H, *J′* = 8.8 Hz, J″ = 2.7 Hz, aromatic), 8.00 (d, 1H, *J* = 8.8 Hz, aromatic); GC–MS *m/z* 253 (M$^+$, 10), 218 (100), 190 (50).

*5.2.2.2. 2-(3-Chloropropyl)-8-methoxy-3,4-dihydroisoquinolin-1(2H)-one (**22**).* Compound **22** was obtained as yellow oil (0.09 g, 30%); $^1$H NMR $\delta$ = 2.10–2.19 (m, 2H, C*H*$_2$CH$_2$Cl), 2.92 (*t*, 2H, *J* = 6.0 Hz, ArCH$_2$), 3.53 (*t*, 2H, *J* = 6.3 Hz, CH$_2$Cl), 3.61–3.70 (m, 4H, 2 CH$_2$N), 3.91 (s, 3H, OCH$_3$), 6.76 (d, 1H, *J* = 7.4 Hz, aromatic), 6.88 (d, 1H, *J* = 8.2 Hz, aromatic), 7.33 (*t*, 1H, *J* = 8.0 Hz, aromatic); GC–MS *m/z* 253 (M$^+$, 78), 218 (100), 204 (44), 190 (58).

*5.2.2.3. 2-(3-Chloropropyl)-6,7-dimethoxy-3,4-dihydroisoquinolin-1(2H)-one (**23**).* Compound **23** was obtained as yellow semi-solid (0.16 g, 46%); mp = 94–96 °C (Litt. mp = 92–95° C) [30]; $^1$H NMR $\delta$ = 2.11–2.15 (m, 2H, C*H*$_2$CH$_2$Cl), 2.93 (*t*, 2H, *J* = 6.3 Hz, ArCH$_2$), 3.48–3.70 (m, 6H, 2 CH$_2$N, and CH$_2$Cl), 3.91 (s, 6H, OCH$_3$), 6.63 (s, 1H, aromatic), 7.57 (s, 1H, aromatic); GC–MS *m/z* 283 (M$^+$, 36), 248 (100), 220 (54).

*5.2.2.4. 2-(3-Chloropropyl)-6-fluoro-3,4-dihydroisoquinolin-1(2H)-one (**24**).* Compound **24** was obtained as colorless oil (0.11 g, 38%); $^1$H NMR $\delta$ = 2.09–2.18 (m, 2H, C*H*$_2$CH$_2$Cl), 3.00 (*t*, 2H, *J* = 6.6 Hz, ArCH$_2$), 3.59–3.69 (m, 6H, 2 CH$_2$N, and CH$_2$Cl), 6.87 (dd, 1H, $J_{HF}$ = 8.8 Hz, $J_{HH}$ = 3 Hz, aromatic), 7.02 (td, 1H, $J_{HF}$ = 8 Hz, $J_{HH}$ = 8.7 Hz, $J_{HH}$ = 3 Hz, aromatic), 8.07 (dd, 1H, $J_{HH}$ = 8.7 Hz, $J_{HF}$ = 5.8 Hz, aromatic); GC–MS *m/z* 241 (M$^+$, 10), 206 (98), 178 (100).

### 5.3. General procedure for the synthesis of final compounds **25**, **26**, **28–31** and intermediate **27**

To a solution of the appropriate alkyl chloride derivative (1.0 mmol) in $CH_3CN$, 6,7-dimethoxy-1,2,3,4-tetrahydroisoquinoline hydrochloride (0.23 g, 1.0 mmol) and $K_2CO_3$ (0.21 g, 1.5 mmol) were added. The mixture was heated to reflux overnight. After cooling to room temperature, the solvent was evaporated to dryness. The residue was treated with $H_2O$ and extracted with $CH_2Cl_2$ (3 × 10 mL) and the collected organic layers, were dried over $Na_2SO_4$ and concentrated under reduced pressure. The crude residue was purified by column chromatography with $CH_2Cl_2$/MeOH (98:2) as eluent.

#### 5.3.1. 2-(3-(6,7-dimethoxy-3,4-dihydroisoquinolin-2(1H)-yl) propyl)-5-methoxy-3,4-dihydroisoquinolin-1(2H)-one (**25**)

Compound **25** was obtained as yellow oil (0.11 g, 28%); $^1$H NMR $\delta$ = 1.85–2.05 (m, 2H, CH$_2$C*H*$_2$CH$_2$), 2.50–3.00 (m, 8H, ArC*H*$_2$-CH$_2$NCO, CH$_2$NCH$_2$CH$_2$Ar), 3.55–3.70 (m, 6H, NCH$_2$Ar, NCO(CH$_2$)$_2$), 3.80 (s, 3H, OCH$_3$), 3.83 (s, 3H, OCH$_3$), 3.85 (s, 3H, OCH$_3$), 6.51 (s, 1H, aromatic), 6.58 (s, 1H, aromatic), 7.00 (d, 1H, *J* = 8.2 Hz, aromatic), 7.22–7.31 (m, 1H, aromatic), 7.70 (d, 1H, *J* = 8.0 Hz, aromatic); LC–MS (ESI$^+$) *m/z*: 411 [M + H]$^+$, 433 [M + Na]$^+$. Anal. ($C_{24}H_{30}N_2O_4 \cdot HCl \cdot H_2O$) C, H, N.

#### 5.3.2. 2-(3-(6,7-Dimethoxy-3,4-dihydroisoquinolin-2(1H)-yl) propyl)-5-(2-fluoroethoxy)-3,4-dihydroisoquinolin-1(2H)-one (**26**)

Compound **26** was obtained as yellow oil (0.11 g, 25%); $^1$H NMR $\delta$ = 1.90–2.00 (m, 2H, CH$_2$C*H*$_2$CH$_2$), 2.59 (*t*, 2H, *J* = 7.5 Hz, CH$_2$CH$_2$C*H*$_2$N), 2.70–3.05 (m, 6H, NCH$_2$CH$_2$Ar and ArC*H*$_2$CH$_2$NCO), 3.54–3.66 (m, 6H, NCH$_2$Ar, NCO(CH$_2$)$_2$), 3.82 (s, 3H, OCH$_3$), 3.85 (s, 3H, OCH$_3$), 4.19 (*t*, 1H, *J* = 4.2 Hz, CH*H*O), 4.28 (*t*, 1H, *J* = 4.0 Hz, C*H*HO), 4.67–4.70 (m, 1H, CH*H*F), 4.83–4.86 (m, 1H, C*H*HF), 6.51 (s,

1H, aromatic), 6.58 (s, 1H, aromatic), 6.95 (d, 1H, $J = 8$ Hz, aromatic), 7.26–7.30 (m, 1H, aromatic), 7.73 (d, 1H, $J = 8$ Hz, aromatic); $^{13}$C NMR: 20.90; 22.58; 24.74; 44.20; 45.89; 50.11; 52.51; 53.27; 55.15; 55.21; 68.00 (d, $^{2}J$ C,$F = 20$ Hz), 81.50 (d, $^{1}J$ C,$F = 168$ Hz); 109.51; 111.35; 115.24; 119.37; 119.54; 119.91; 123.04; 127.31; 127.71; 129.52; 148.60; 149.43; 154.79; 166.07. LC-–MS (ESI$^+$) *m/z* 443 [M + H]$^+$; LC–MS–MS 443: 250, 222; Anal. ($C_{25}H_{31}FN_2O_4 \cdot HCl \cdot 1.5H_2O$) C, H, N.

*5.3.3. 2-(3-(6,7-Dimethoxy-3,4-dihydroisoquinolin-2(1H)-yl) propyl)-5-benzyloxy-3,4-dihydroisoquinolin-1(2H)-one (**27**)*

Compound **27** was obtained as brown oil (0.19 g, 40%); $^1$H NMR $\delta$ = 1.90–2.05 (m, 2H, $CH_2CH_2CH_2N$), 2.57–3.05 (m, 8H, $ArCH_2$-$CH_2NCOCH_2CH_2CH_2NCH_2CH_2Ar$), 3.48–3.70 (m, 6H, $CON(CH_2)_2$, $ArCH_2N$), 3.82 (s, 3H, $OCH_3$), 3.83 (s, 3H, $OCH_3$), 5.05 (s, 2H, $PhCH_2O$), 6.48 (s, 1H, aromatic), 6.58 (s, 1H, aromatic), 7.02 (d, 1H, $J = 8.0$ Hz, aromatic), 7.30–7.45 (m, 6H, aromatic), 7.72 (d, 1H, $J = 7.7$ Hz, aromatic); GC/MS *m/z* 486 (M$^{+\cdot}$, 0.5), 192 (100); LC–MS (ESI$^+$) *m/z*: 487 [M + H]$^+$, 509 [M + Na]$^+$; LC–MS–MS: 403.

*5.3.4. 2-(3-(6,7-Dimethoxy-3,4-dihydroisoquinolin-2(1H)-yl) propyl)-6-methoxy-3,4-dihydroisoquinolin-1(2H)-one (**28**)*

Compound 28 was obtained as colorless oil (0.12 g, 29%); $^1$H NMR $\delta$ = 1.76–1.98 (m, 2H, $CH_2CH_2CH_2$), 2.58–3.00 (m, 8H, $ArCH_2CH_2NCO$, $CH_2NCH_2CH_2Ar$), 3.55–3.65 (m, 6H, $NCH_2Ar$, $NCO(CH_2)_2$), 3.82 (s, 3H, $OCH_3$), 3.83 (s, 6H, 2 $OCH_3$), 6.51 (s, 1H, aromatic), 6.58 (s, 1H, aromatic), 6.65 (d, 1H, $J = 2.2$ Hz, aromatic), 6.84 (dd, 1H, $J'' = 8.8$ Hz, $J' = 2.5$ Hz, aromatic), 8.01 (d, 1H, $J = 8.8$ Hz, aromatic); $^{13}$C NMR: 22.76; 24.95; 27.89; 44.11; 46.46; 50.23; 52.63; 53.37; 54.82; 55.26; 55.31; 109.55; 111.43; 111.92; 112.70; 119.54; 121.02; 123.19; 129.77; 141.33; 148.70; 149.51; 163.37; 166.48. GC/MS *m/z* 410 (M$^{+\cdot}$, 1.2), 192 (100); LC–MS (ESI$^+$) *m/z*: 411 [M + H]$^+$, 433 [M + Na]$^+$. Anal. ($C_{24}H_{30}N_2O_4 \cdot HCl \cdot H_2O$) C, H, N.

*5.3.5. 2-(3-(6,7-Dimethoxy-3,4-dihydroisoquinolin-2(1H)-yl) propyl)-8-methoxy-3,4-dihydroisoquinolin-1(2H)-one (**29**)*

Compound 29 was obtained as yellow oil (0.041 g, 10%); $^1$H NMR $\delta$ = 1.80–2.00 (m, 2H, $CH_2CH_2CH_2N$), 2.55–2.95 (m, 8H, $ArCH_2$, $CH_2NCH_2CH_2Ar$), 3.45–3.65 (m, 6H, $NCH_2Ar$, $NCO(CH_2)_2$), 3.82 (s, 3H, $OCH_3$), 3.85 (s, 3H, $OCH_3$), 3.91 (s, 3H, $OCH_3$), 6.51 (s, 1H, aromatic), 6.58 (s, 1H, aromatic), 6.74 (d, 1H, $J = 7.4$ Hz, aromatic), 6.87 (d, 1H, $J = 8.2$ Hz, aromatic), 7.32 (*t*, 1H, $J = 8.2$ Hz, aromatic); GC/MS *m/z* 410 (M$^{+\cdot}$, 1), 192 (100); LC–MS (ESI$^+$) *m/z*: 433 [M + Na]$^+$. HPLC analysis using acetonitrile/20 mM $NH_4COOH$ (65:35 v/v), at a flow rate 1 mL/min indicated the compound was >98% pure.

*5.3.6. 2-(3-(6,7-Dimethoxy-3,4-dihydroisoquinolin-2(1H)-yl) propyl)-6,7-dimethoxy-3,4-dihydroisoquinolin-1(2H)-one (**30**)*

Compound 30 was obtained as yellow oil (0.10 g, 25%); $^1$H NMR $\delta$ = 1.91–2.00 (m, 2H, $CH_2CH_2CH_2$), 2.59–2.95 (m, 8H, $CH_2NCH_2CH_2Ar$ and $ArCH_2CH_2NCO$), 3.54–3.58 (m, 6H, $NCH_2Ar$, $NCO(CH_2)_2$), 3.82 (s, 3H, $OCH_3$), 3.85 (s, 3H, $OCH_3$), 3.91 (s, 6H, $OCH_3$), 6.51 (s, 1H, aromatic), 6,60 (s, 1H, aromatic), 6.62 (s, 1H, aromatic), 7.59 (s, 1H, aromatic); $^{13}$C NMR: 22.81; 24.90; 27.15; 44.25; 46.67; 50.23; 52.60; 53.42; 55.26; 55.32; 55.38; 109.57; 109.90; 110.33; 111.41; 119.49; 120.710; 123.17; 133.29; 148.42; 148.68; 149.51; 152.99; 166.37. LC–MS (ESI$^+$) *m/z*: 441 [M + H]$^+$, 463 [M + Na]$^+$. Anal. ($C_{25}H_{32}N_2O_5 \cdot HCl \cdot ½H_2O$) C, H, N.

*5.3.7. 2-(3-(6,7-Dimethoxy-3,4-dihydroisoquinolin-2(1H)-yl) propyl)-6-fluoro-3,4-dihydroisoquinolin-1(2H)-one (**31**)*

Compound **31** was obtained as yellow oil (0.11 g, 27%); $^1$H NMR $\delta$ = 1.90–2.00 (m, 2H, $CH_2CH_2CH_2$), 2.59 (*t*, 2H, $J$ = 7.3 Hz, $CH_2CH_2CH_2N$), 2.70–3.00 (m, 6H, $NCH_2CH_2Ar$ and $ArCH_2CH_2NCO$), 3.56–3.66 (m, 6H, $NCH_2Ar$, $NCO(CH_2)_2$), 3.82 (s, 3H, $OCH_3$), 3.83 (s, 3H, $OCH_3$), 6.58 (s, 1H, aromatic), 6.63 (s, 1H, aromatic), 6.86 (dd, 1H, $J_{HF} = 8.8$ Hz, $J_{HH} = 2.2$ Hz, aromatic), 7.00 (td, 1H, $J_{HF} = 8.0$ Hz, $J_{HH} = 8.7$ Hz, $J_{HH} = 2.5$ Hz, aromatic), 8.00–8.10 (m, 1H, aromatic); GC–MS *m/z* 398 (M$^+$, 2), 192 (100); Anal. ($C_{23}H_{27}FN_2O_3 \cdot HCl \cdot H_2O$) C, H, N.

*5.3.8. 2-(3-(6,7-Dimethoxy-3,4-dihydroisoquinolin-2(1H)-yl) propyl)-5-hydroxy-3,4-dihydroisoquinolin-1(2H)-one (**32**)*

A solution of benzyl derivative **27** (0.4 mmol, 0.19 g) in $CH_3OH$ (10 mL) was added with Pd on 10% activated carbon and hydrogenated for 6 h. After filtration of the catalyst on Celite pad and the filtrate was concentrated under reduced pressure to afford the target compound as yellow oil (0.16 g, 100%); LC–MS (ESI$^-$) *m/z*: 395 [M − H]$^-$; IR cm$^{-1}$: 3182, 3055, 2936, 1667, 1644.

*5.3.9. 2-(3-(6,7-Dimethoxy-3,4-dihydroisoquinolin-2(1H)-yl) propyl)-5-(2-acetoxy-ethoxy)-3,4-dihydroisoquinolin-1(2H)-one (**33**)*

A solution of **32** (0.54 mmol, 0.22 g) in acetone (30 mL) (which was warmed to improve the solubility of the compound) was added with 2-bromoethylacetate (3.56 mmol, 0.4 mL) and $K_2CO_3$ (3.56 mol, 0.50 g) and refluxed overnight. The mixture was evaporated under reduced pressure and the residue taken up with $H_2O$ and extracted with ethyl acetate (3 × 20 mL). The collected organic layers were dried over $Na_2SO_4$ and evaporated under reduced pressure. The crude residue was purified by column chromatography with $CH_2Cl_2/CH_3OH$ (95:5) as eluent to give the target compound as yellow oil (0.12 g, 46%); LC–MS (ESI$^+$) *m/z*: 483 [M + H]$^+$; 505 [M + Na]$^+$.

*5.3.10. 2-(3-(6,7-Dimethoxy-3,4-dihydroisoquinolin-2(1H)-yl) propyl)-5-(2-hydroxy-ethoxy)-3,4-dihydroisoquinolin-1(2H)-one (**34**)*

NaOH (0.52 mmol, 0.02 g) was added to a solution of intermediate **33** (0.26 mmol, 0.12 g) in $CH_3OH$ (12 mL) and $H_2O$ (6.0 mL) and the mixture was stirred overnight. HCl 2 N was added to neutralize the solution and the solvent was evaporated under reduced pressure to afford a residue that was taken up with water and then extracted with ethyl acetate (3 × 10 mL). The collected organic layers were dried over $Na_2SO_4$ and evaporated under reduced pressure. The crude residue was purified by column chromatography with $CH_2Cl_2/CH_3OH$ (9:1) as eluent to give the target compound as yellow oil (0.08 g, 70%); LC–MS (ESI$^+$) *m/z*: 441 [M + H]$^+$; 463 [M + Na]$^+$, LC–MS–MS 441: 248.

*5.3.11. 2-(3-(6,7-Dimethoxy-3,4-dihydroisoquinolin-2(1H)-yl) propyl)-5-(2-ethyltosylate)-3,4-dihydroisoquinolin-1(2H)-one (**35**)*

A solution of **34** (0.18 mmol, 0.08 g) in $CH_2Cl_2$ kept at 0 °C was added with Tosyl chloride (0.21 mmol, 0.040 g) and $NEt_3$ (0.21 mmol, 0.0027 mL). The mixture was kept under stirring at room temperature for 1 h, then added with $NH_4Cl$ and extracted with $CH_2Cl_2$ (3 × 10 mL). The collected organic layers were dried over $Na_2SO_4$ and evaporated under reduced pressure. The crude residue was purified by column chromatography with $CH_2Cl_2/CH_3OH$ (95:5) as eluent to give the target compound as pale yellow oil (0.069 g, 65%); LC–MS (ESI$^+$) *m/z*: 595 [M + H]$^+$; 617 [M + Na]$^+$, LC–MS–MS 595: 402.

## 6. Biological materials and methods

### *6.1. Materials*

Human recombinant serotonin 5-HT$_7$ receptors expressed in CHO–K1 cells, human recombinant serotonin 5-HT$_{1A}$ receptors

expressed in HEK293-EBNA cells, [$^3$H]-DTG, (+)-[$^3$H]-pentazocine, [$^3$H]-5-CT, [$^3$H]-8-OH-DPAT and [$^3$H]-Prazosin were obtained from PerkinElmer Life and Analytical Sciences (Boston, MA, USA). DTG and 5-CT were purchased from Tocris Bioscience (Bristol, UK). (+)-Pentazocine, 8-OH-DPAT hydrobromide, phentolamine hydrochloride, and Calcein-AM were from Sigma–Aldrich (Milan, Italy). Male Dunkin guinea-pigs and Wistar Hannover rats (250–300 g) were from Harlan, Italy. Cell culture reagents were purchased from EuroClone (Milan, Italy).

### 6.2. $\sigma_1$ and $\sigma_2$ radioligand binding assays

All the procedures for the binding assays were previously described. $\sigma_1$ And $\sigma_2$ receptor binding were carried out according to Matsumoto et al. [31]. The specific radioligands and tissue sources were respectively: (a) $\sigma_1$ receptor, (+)-[$^3$H]-pentazocine, guinea-pig brain membranes without cerebellum; (b) $\sigma_2$ receptor, [$^3$H]-DTG in the presence of 1 μM (+)-pentazocine to mask $\sigma_1$ receptors, rat liver membranes. The following compounds were used to define the specific binding reported in parentheses: (a) (+)-pentazocine (73–87%), (b) DTG (85–96%). Concentrations required to inhibit 50% of radioligand specific binding ($IC_{50}$) were determined by using six to nine different concentrations of the drug studied in two or three experiments with samples in duplicate. Scatchard parameters ($K_d$ and $B_{max}$) and apparent inhibition constants ($K_i$) values were determined by nonlinear curve fitting, using the Prism, version 3.0, GraphPad software [32].

### 6.3. 5-HT$_7$ radioligand binding assay

Binding of [$^3$H]-5-CT at human cloned 5-HT$_7$ receptor was performed according to Jasper et al. [33] with minor modifications. In 0.5 mL of incubation buffer (50 mM Tris–HCl, 10 mM $MgSO_4$ and 0.5 mM EDTA, pH 7.4) were suspended 34 μg of membranes, 1.5 nM [$^3$H]-5-CT, the drugs or reference compound (six to nine concentrations). The samples were incubated for 120 min at 27 °C. The incubation was stopped by rapid filtration on Whatman GF/C glass microfiber filters (pre-soaked in 0.3% polyethylenimine for 30 min). The filters were washed with 3 × 1 mL of ice-cold buffer (50 mM Tris–HCl, pH 7.4). Nonspecific binding was determined in the presence of 10 μM 5-CT. Approximately 90% of specific binding was determined under these conditions.

### 6.4. 5-HT$_{1A}$ radioligand binding assay

Human 5-HT$_{1A}$ serotonin receptors stably expressed in HEK293-EBNA cells were radiolabelled with 1.0 nM [$^3$H]-8-OH-DPAT [34]. Samples containing 32 μg of membrane protein, different concentrations of each compound ranging from 0.1 nM to 10 μM were incubated in a final volume of 500 μL of 50 mM Tris–HCl pH 7.4, 5 mM $MgSO_4$ for 120 min at 37 °C. After this incubation time, samples were filtered through Whatman GF/C glass microfiber filters pre-soaked in polyethylenimine 0.5% for at least 30 min prior to use. The filters were washed twice with 1 mL of ice-cold buffer (50 mM Tris–HCl, pH 7.4). Nonspecific binding was determined in the presence of 10 μM 5-HT.

### 6.5. $\alpha_1$ adrenoceptors radioligand binding assay

Binding experiments were performed according to Glossman and Hornung with minor modifications [35]. Each tube received, in a final volume of 1 mL, incubation buffer (50 mM Tris–HCl pH 7.4, 120 mM NaCl, 5 mM KCl, 5 mM $CaCl_2$, 1 mM $MgCl_2$), 500 μg rat cerebral cortex membranes and 1 nM [$^3$H]-Prazosin. For competitive inhibition experiments various concentrations of the drugs studied were incubated. Nonspecific binding was defined using 10 μM phentolamine. Samples were incubated at 25 °C for 50 min and then filtered on Whatman GF/C glass microfiber filters presoaked in polyethylenimine 0.5% for 50 min. The filters were washed twice with 2 mL of ice-cold buffer (50 mM Tris–HCl, pH 7.4).

## 7. Radiochemistry

No-carrier-added (n.c.a) $^{18}$F-fluoride was produced via the $^{18}$O(p,n)$^{18}$F nuclear reaction in a fixed-energy Cyclone 18/9 cyclotron (IBA, Belgium) by irradiating >98% isotopically enriched $^{18}$O-water (Nukem GmbH, Germany) by 18 MeV proton beam. Produced $^{18}$F-fluoride/$^{18}$O-water solution was transferred using a helium stream from the target to a shielded hot cell equipped with a manipulator, where radiosynthesis was performed. $^{18}$F-fluoride was trapped on an anion exchange Sep-Pak Light Accell Plus QMA cartridge (Waters) preconditioned with 5 mL 0.5 M potassium carbonate solution, 10 mL water and flushed with 10 mL air. It was eluted with 1 mL solution of potassium carbonate (1 mg) and Kryptofix K2.2.2 (5 mg) in acetonitrile/water (4:1 v/v). Effluent was collected to a tightly closed 5 mL Reacti-Vial (Thermo Fisher Scientific) and solvent was evaporated under a stream of nitrogen and reduced pressure (50–80 mbar) at 95 °C. The residue was azeotropically dried by addition of 3 × 0.8 mL anhydrous acetonitrile. Precursor **35** (2.4 mg, 4 μmol) predissolved in 300 μL anhydrous acetonitrile was added to the dry $^{18}$F-fluoride and the reaction mixture was heated at 100 °C for 10 min. After cooling for 5 min at room temperature the reaction mixture was diluted with 2 mL acetonitrile/50 mM $NH_4COOH$ (1:1 v/v) and loaded into semi-preparative HPLC. The radioactive fraction containing the product was collected into 30 mL water and passed through a Sep-Pak Light C18 cartridge (preconditioned with 5 mL ethanol followed by 10 mL water). The cartridge was washed with additional 5 mL water for injection. The product was eluted with 0.5 mL ethanol to a penicillin vial and diluted with 9.5 mL 0.9% sodium chloride solution. An aliquot of known volume and radioactivity of the final formulated solution was injected into analytical HPLC for the quality control. The specific radioactivity was determined matching the area of the UV absorbance peak at 235 nm, which co-eluted with the radiolabeled product, to a standard calibration curve calculated using known concentrations (0.5–20 μg/ml) of the non-radioactive reference compound **26**.

## 8. Animal care

Animal care and all experimental procedures were according to Swiss Animal Protection legislation and approved by the Veterinary Office of the Canton Zurich. Male Wistar rats were purchased from (Charles River, Sulzfeld, Germany) and were allowed free access to food and water.

## 9. In vitro autoradiography

A male Wistar rat was sacrificed by decapitation under isoflurane anesthesia. The brain was removed, frozen, and cut in horizontal slices (20 μm) at −20 °C using a MICROM microtome cryostat HM 505 N. The brain slices were mounted on SuperFrost Plus slides (Menzel, Thermo Fisher Scientific) and stored at −80 °C. The slices were thawed at room temperature (rt) for 30 min before the experiment and incubated in 50 mM TRIS-HCl buffer (pH 7.4) at 4 °C for 10 min. A solution of [$^{18}$F]-**26** (9 nM in TRIS-HCl containing 1% bovine serum albumin, BSA) was pipetted on the brain slices ($n = 4$). Another three sets of brain slices ($n = 4$) were incubated with the [$^{18}$F]-**26** solution containing either, 0.9 μM unlabeled **26**,

90 μM unlabeled **26**, or 90 μM haloperidol. After 45 min incubation at rt, the slides were washed with TRIS-HCl/BSA and twice with TRIS-HCl for 3 min each and then rinsed twice with distilled water. The sections were air-dried and exposed to a BAS-TR 2025 phosphor imaging plate (Raytest Fuji). After 15 min exposure time the imaging plates were scanned in a BAS-5000 bio-imaging analyzer (Fujifilm). Data were analyzed and processed with the AIDA 4.5 software (Raytest Fuji).

## 10. PET imaging

Male Wistar rats were anesthetized by isoflurane inhalation using an oxygen/air mixture as carrier gas. One rat (302 g) was injected with 47 MBq (0.8 nmol) [$^{18}$F]-**26** into a tail vein and the head was scanned in a GE eXplore VISTA PET/CT tomograph (axial field of view 4.8 cm) in PET list mode from 0 to 90 min after injection, followed by a CT scan for anatomical orientation. A second rat (291 g) was injected into a tail vein 1 mg/kg haloperidol immediately before tracer injection and scanned as above (34 MBq, 1.3 nmol). Raw data were reconstructed in user-defined time frames (5 × 2, 6 × 5, 2 × 10 min) with a voxel size of 0.3875 × 0.3875 × 0.775 mm$^3$ by 2D-ordered subsets expectation-maximization (2D-OSEM). Random and singlet but no attenuation correction was applied. Image files were evaluated by region of interest (ROI) analysis using PMOD software (PMOD Technologies, Switzerland) and standardized uptake values (SUV) were calculated from the image-derived radioactivity per cm$^3$ tissue (Bq/cm$^3$) normalized by the injected radioactivity dose per g body weight (Bq/g).

## Acknowledgments

We thank Claudia Keller and Martin Hungerbühler for the excellent technical help in conducting in vitro and in vivo experiments, and Dr. Marialessandra Contino and Dr. Maria Grazia Perrone for performing Calcein-AM and permeability assays.

## Appendix A. Supplementary data

Supplementary data related to this article can be found at http://dx.doi.org/10.1016/j.ejmech.2013.09.018.

## References

[1] M. Hanner, F.F. Moebius, A. Flandorfer, H.G. Knaus, J.M. Striessnig, E. Kempner, H. Glossmann, Purification, molecular cloning, and expression of the mammalian sigma1-binding site, Proc. Natl. Acad. Sci. 93 (1996) 8072–8077.
[2] T. Hayashi, T.P. Su, Sigma-1 receptor chaperones at the ER-mitochondrion interface regulate $Ca^{2+}$ signaling and cell survival, Cell 131 (2007) 596–610.
[3] E.J. Cobos, J.M. Entrena, F.R. Nieto, C.M. Cendan, E. Del Pozo, Pharmacology and therapeutic potential of sigma$_1$ receptor ligands, Curr. Neuropharmacol. 6 (2008) 344–366.
[4] C. Abate, J. Elenewski, M. Niso, F. Berardi, N.A. Colabufo, A. Azzariti, R. Perrone, R.A. Glennon, Interaction of the $\sigma_2$ receptor ligand PB28 with the human nucleosome: computational and experimental probes of interaction with the H2A/H2B dimer, Chem. Med. Chem. 5 (2010) 268–273.
[5] J. Xu, C. Zeng, W. Chu, F. Pan, J.M. Rothfuss, F. Zhang, Z. Tu, D. Zhou, D. Zeng, S. Vangveravong, F. Johnston, D. Spitzer, K.C. Chang, R.S. Hotchkiss, W.G. Hawkins, K.T. Wheeler, R.H. Mach, Identification of the PGRMC1 protein complex as the putative sigma-2 receptor binding site, Nat. Commun. 2 (2011) 380.
[6] S.U. Mir, I.S. Ahmed, S. Arnold, R.J. Craven, Elevated progesterone receptor membrane component 1/sigma-2 receptor levels in lung tumors and plasma from lung cancer patients, Int. J. Cancer 131 (2012) E1–E9.
[7] C. Abate, R. Perrone, F. Berardi, Classes of sigma$_2$ ($\sigma_2$) receptor ligands: structure affinity relationship (SAfiR) studies and antiproliferative activity, Curr. Pharm. Des. 18 (2012) 938–949.
[8] A. van Waarde, A.A. Rybczynska, N. Ramakrishnan, K. Ishiwata, P.H. Elsinga, R.A. Dierckx, Sigma receptors in oncology: therapeutic and diagnostic applications of sigma ligands, Curr. Pharm. Des. 16 (2010) 3519–3537.
[9] D. Spitzer, P.O. Simon Jr., H. Kashiwagi, J. Xu, C. Zeng, S. Vangveravong, D. Zhou, K. Chang, J.E. McDunn, J.R. Hornick, P. Goedegebuure, R.S. Hotchkiss, R.H. Mach, W.G. Hawkins, Use of multifunctional sigma-2 receptor ligand conjugates to trigger cancer-selective cell death signaling, Cancer Res. 72 (2012) 201–209.
[10] C. Zeng, J. Rothfuss, J. Zhang, W. Chu, S. Vangveravong, Z. Tu, F. Pan, K.C. Chang, R. Hotchkiss, R.H. Mach, Sigma-2 ligands induce tumour cell death by multiple signalling pathways, Br. J. Cancer 106 (2012) 693–701.
[11] J.R. Hornick, J. Xu, S. Vangveravong, Z. Tu, J.B. Mitchem, D. Spitzer, P. Goedegebuure, R.H. Mach, W.G. Hawkins, The novel sigma-2 receptor ligand SW43 stabilizes pancreas cancer progression in combination with gemcitabine, Mol. Cancer 9 (2010) 298.
[12] J.R. Hornick, S. Vangveravong, D. Spitzer, C. Abate, F. Berardi, P. Goedegebuure, R.H. Mach, W.G. Hawkins, Lysosomal membrane permeabilization is an early event in sigma-2 receptor ligand mediated cell death in pancreatic cancer, J. Exp. Clin. Cancer Res. 31 (2012) 41.
[13] H. Kashiwagi, J.E. McDunn, P.O. Simon Jr., P. Goedegebuure, S. Vangveravong, K.C. Chang, R. Hotchkiss, R.H. Mach, W.G. Hawkins, Sigma-2 receptor ligands potentiate conventional chemotherapies and improve survival in models of pancreatic adenocarcinoma, J. Transl. Med. 7 (2009) 24.
[14] K.T. Wheeler, L.M. Wang, C.A. Wallen, S.R. Childers, J.M. Cline, P.C. Keng, R.H. Mach, Sigma-2 receptors as a biomarker of proliferation in solid tumours, Br. J. Cancer 82 (2000) 1223–1232.
[15] Phase I Clinical Trial. ClinicalTrials.gov Identifier: NCT00968656. Assessment of Cellular Proliferation in Tumors by Positron Emission Tomography (PET) using [$^{18}$F]ISO-1 (FISO PET/CT)
[16] R.H. Mach, K.T. Wheeler, Development of molecular probes for imaging sigma-2 receptors in vitro and in vivo, Cent. Nerv. Syst. Agents Med. Chem. 9 (2009) 230–245.
[17] R.H. Mach, Y. Huang, R.A. Freeman, L. Wu, S. Vangveravong, R.R. Luedtke, Conformationally-flexible benzamide analogues as dopamine D3 and sigma 2 receptor ligands, Bioorg. Med. Chem. Lett. 14 (2004) 195–202.
[18] F. Berardi, S. Ferorelli, C. Abate, N.A. Colabufo, M. Contino, R. Perrone, V. Tortorella, 4-(Tetralin-1-yl)- and 4-(naphthalen-1-yl)alkyl derivatives of 1-cyclohexylpiperazine as sigma receptor ligands with agonist sigma2 activity, J. Med. Chem. 47 (2004) 2308–2317.
[19] F. Berardi, C. Abate, S. Ferorelli, N.A. Colabufo, R. Perrone, 1-Cyclohexylpiperazine and 3,3-dimethylpiperidine derivatives as sigma-1 ($\sigma_1$) and sigma-2 ($\sigma_2$) receptor ligands: a review, Cent. Nerv. Syst. Agents Med. Chem. 9 (2009) 205–219.
[20] C. Abate, S. Ferorelli, M. Contino, R. Marottoli, N.A. Colabufo, R. Perrone, F. Berardi, Arylamides hybrids of two high-affinity $\sigma_2$ receptor ligands as tools for the development of PET radiotracers, Eur. J. Med. Chem. 46 (2011) 4733–4741.
[21] M. Gao, M. Wang, K.D. Miller, G.W. Sledge, Q.H. Zheng, Synthesis and preliminary biological evaluation of new carbon-11 labeled tetrahydroisoquinoline derivatives as SERM radioligands for PET imaging of ER expression in breast cancer, Eur. J. Med. Chem. 43 (2008) 2211–2219.
[22] M.D. Meyer, J.F. De Bernardis, A.A. Hancock, Synthesis and structure activity relationships of cis- and trans-2,3,4,4a,9,9a-hexahydro-1H-indeno [2,1-c]pyridines for 5-HT receptor subtypes, J. Med. Chem. 37 (1994) 105–112.
[23] C.D. Jesudason, L.S. Beavers, J.W. Cramer, J. Dill, D.R. Finley, C.W. Lindsley, F.C. Stevens, R.A. Gadski, S.W. Oldham, R.T. Pickard, C.S. Siedem, D.K. Sindelar, A. Singh, B.M. Watson, P.A. Hipskind, Synthesis and SAR of novel histamine H3 receptor antagonists, Bioorg. Med. Chem. Lett. 16 (2006) 3415–3418.
[24] I.A. Moussa, S.D. Banister, C. Beinat, N. Giboureau, A.J. Reynolds, M. Kassiou, Design, synthesis, and structure-affinity relationships of regioisomeric *N*-benzyl alkyl ether piperazine derivatives as sigma-1 receptor ligands, J. Med. Chem. 53 (2010) 6228–6239.
[25] Y. Miyake, H. Shimadzu, N. Hashimoto, Y. Ishida, M. Shibakawa, T. Nishimura, Synthesis of 3,4-dihydro-5-[$^{11}$C]methoxy-1(2H)-isoquinolinone as a potential tracer of poly(ADP-ribose)synthetase, J. Labelled Compd. Radiopharm. 43 (2000) 983–988.
[26] R. Pellicciari, E. Camaioni, G. Costantino, L. Formentini, P. Sabbatini, F. Venturoni, G. Eren, D. Bellocchi, A. Chiarugi, F. Moroni, On the way to selective PARP-2 inhibitors. Design, synthesis, and preliminary evaluation of a series of isoquinolinone derivatives, ChemMedChem 3 (2008) 914–923.
[27] K.K. Søby, J.D. Mikkelsen, E. Meier, C. Thomsen, Lu 28-179 labels a sigma(2)-site in rat and human brain, Neuropharmacology 43 (2002) 95–100.
[28] ACD Labs, Version 7.07, Advanced Chemistry Development Inc, Toronto, Canada, 2003.
[29] Sovicell, TRANSIL_XL PBB binding kit, Version 2, Revision 00.
[30] M. Reiffen, W. Eberlein, P. Mueller, M. Psiorz, K. Noll, J. Heider, C. Lillie, W. Kobinger, P. Luger, Specific bradycardic agents. 1. Chemistry, pharmacology, and structure-activity relationships of substituted benzazepinones, a-new class of compounds exerting antiischemic properties, J. Med. Chem. 33 (1990) 1496–1504.
[31] R.R. Matsumoto, W.D. Bowen, M.A. Tom, D.D. Truong, B.R. De Costa, Characterization of two novel sigma receptor ligands: antidystonic effects in rats suggest sigma receptor antagonism, Eur. J. Pharmacol. 280 (1995) 301–310.

[32] Prism Software, Version 3.0 for Windows, GraphPad Software, Inc., San Diego, CA, 1998.
[33] J.R. Jasper, A. Kosaka, Z.P. To, D.J. Chang, R.M. Eglen, Cloning, expression and pharmacology of a truncated splice variant of the human 5-$HT_7$ receptor (h5-$HT_{7b}$), Br. J. Pharmacol. 122 (1997) 126–132.
[34] A. Fargin, J.R. Raymond, J.W. Regan, S. Cotecchia, R.J. Lefkowitz, M.G. Caron, Effector coupling mechanisms of the cloned 5-HT1A receptor, J. Biol. Chem. 264 (1989) 14848–14852.
[35] H. Glossmann, R. Hornung, α-Adrenoceptors in rat brain: sodium changes the affinity of agonists for prazosin sites, Eur. J. Pharmacol. 61 (1980) 407–408.